Biosensors and Bioelectronics 86 (2016) 770–776

Contents lists available at ScienceDirect

Biosensors and Bioelectronics

journal homepage: www.elsevier.com/locate/bios

# Fast and sensitive detection of foodborne pathogen using electrochemical impedance analysis, urease catalysis and microfluidics

Qi Chen [a], Dan Wang [a], Gaozhe Cai [a], Yonghua Xiong [b], Yuntao Li [c], Maohua Wang [d], Huiling Huo [e], Jianhan Lin [a,*]

[a] MOA Key Laboratory of Agricultural Information Acquisition Technology (Beijing), China Agricultural University, Beijing, China
[b] State Key Laboratory of Food Science and Technology, Nanchang University, Nanchang, China
[c] State Key Lab of Integrated Optoelectronics, Institute of Semiconductors, Chinese Academy of Science, Beijing, China
[d] Modern Precision Agriculture System Integration Research Key Laboratory of Ministry of Education, China Agricultural University, Beijing, China
[e] Hebei Province Institute of Veterinary Drug Control, Shijiazhuang, China

ARTICLE INFO

*Article history:*
Received 29 April 2016
Received in revised form
20 July 2016
Accepted 21 July 2016
Available online 22 July 2016

*Keywords:*
Microfluidic impedance biosensor
Phase angle
Urease catalysis
Immunomagnetic separation
*Listeria monocytogenes*

ABSTRACT

Early screening of pathogenic bacteria is a key to prevent and control of foodborne diseases. In this study, we developed a fast and sensitive bacteria detection method integrating electrochemical impedance analysis, urease catalysis with microfluidics and using *Listeria* as model. The *Listeria* cells, the anti-*Listeria* monoclonal antibodies modified magnetic nanoparticles (MNPs), and the anti-*Listeria* polyclonal antibodies and urease modified gold nanoparticles (AuNPs) were incubated in a fluidic separation chip with active mixing to form the MNP-*Listeria*-AuNP-urease sandwich complexes. The complexes were captured in the separation chip by applying a high gradient magnetic field, and the urea was injected to resuspend the complexes and hydrolyzed under the catalysis of the urease on the complexes into ammonium ions and carbonate ions, which were transported into a microfluidic detection chip with an interdigitated microelectrode for impedance measurement to determine the amount of the *Listeria* cells. The capture efficiency of the *Listeria* cells in the separation chip was ~93% with a shorter time of 30 min due to the faster immuno-reaction using the active magnetic mixing. The changes on both impedance magnitude and phase angle were demonstrated to be able to detect the *Listeria* cells as low as $1.6 \times 10^2$ CFU/mL. The detection time was reduced from original ~2 h to current ~1 h. The recoveries of the spiked lettuce samples ranged from 82.1% to 89.6%, indicating the applicability of this proposed biosensor. This microfluidic impedance biosensor has shown the potential for online, automatic and sensitive bacteria separation and detection.



## 1. Introduction

Food safety caused by foodborne pathogens has shown a great threaten to public health worldwide. The US CDC estimated that major known pathogens and unspecified agents transmitted by foods resulted in a total cost of US$ 78 billion annually (Mclinden et al., 2014; Scharff, 2012). In China, pathogenic microorganisms have been reported to be responsible for over 50% of foodborne illnesses since 2006 (Xue and Zhang, 2013). Thus, early screening of foodborne pathogens is the key to prevent and control the outbreaks of foodborne diseases. Current methods for foodborne pathogen detection mainly include traditional culture plating (gold standard method), polymerase chain reaction (PCR), enzyme-linked immuno-sorbent assay (ELISA) and immuno-chromatographic lateral flow assay (strip). However, these methods either require long time to obtain final results (culture), or need complex nucleic acid extraction procedures and expensive instruments (PCR), or have relatively high false positives (ELISA), or lack sensitivity and specificity (strip). Therefore, sensitive, rapid and low-cost methods for the detection of foodborne pathogens are needed for food safety.

In the past decade, many efforts have been made by scientists to develop new methods for rapid detection of foodborne pathogens. As alternatives, various biosensors have been reported with shorter detection time (Hernandez et al., 2014; Lee et al., 2014), higher sensitivity (Larou et al., 2013; Lee et al., 2014), simpler operation(Chen et al., 2011), and lower cost (Lin et al., 2015) using nano-materials (Liu et al., 2013; Tang et al., 2016; Wang et al., 2012), enzymes(Chen et al., 2015; Miranda et al., 2011) or chemical reagents (Sun et al., 2011; Wang and Liu, 2009) as signal amplifiers or carriers.

Impedance biosensors rely on electrochemical changes on the

* Corresponding author.
*E-mail address:* jianhan@cau.edu.cn (J. Lin).

http://dx.doi.org/10.1016/j.bios.2016.07.071
0956-5663/

electrode's surface during the detection of an analyte and have shown some advantages over traditional methods for bacteria detection, such as compact design, low cost and rapid response. Impedance biosensors often use interdigitated microelectrodes (IMEs) as transducer to obtain higher sensitivity and faster detection since IMEs are featured with low ohmic drop, rapid reaction kinetics, high signal-to-noise ratio, and miniature size. Recently, some impedance biosensors integrated with microfluidics were developed for the detection of foodborne pathogens, which offered higher surface-to-volume ratio, better small-volume sample handling capability, shorter detection time, automatic operation, and free cross-contamination. In these microfluidic impedance biosensors, the biological recognition elements were immobilized on the surface of the electrodes, which could capture the bacteria by antigen-antibody reaction resulting in the impedance changes on the electrode-solution interface (Ghosh Dastider et al., 2015a; Varshney and Li, 2009). However, their reproducibility was often unsatisfied due to the complicated electrode modification procedure, and the capture efficiency was often relatively low due to solid-liquid phase reaction, which limited their practical applications (Ghosh Dastider et al., 2015b). Besides, the volume of the sample for bacteria detection in the microfluidic biosensors is very small, generally at microliter or nanoliter level. Even if the biosensors could detect the bacteria as low as one cell, i.e., their lower detection limits were 1 CFU/μL or 1 CFU/nL, equal to $10^3$ CFU/mL or $10^6$ CFU/mL, they still were not sensitive enough for foodborne pathogen detection because most of them should not be found in food samples (Kanayeva et al., 2012).

In our recent study, we reported an impedance biosensor combining immunomagnetic separation with urease catalysis for detection of *Listeria* using an immobilization-free interdigitated array microelectrode. The previously reported biosensor was demonstrated to be capable to detect *Listeria* in food samples with a lower detection limit of $3 \times 10^2$ CFU/mL in 2 h. The relatively high sensitivity of this biosensor was originated from quantitative determination of the catalysate (ammonium ions and carbonate ions) at very low concentrations using the microelectrode to measure its impedance change. Thus, this biosensor had to perform tedious washing steps very carefully to eliminate the background noise because it was susceptible for the conductivity of the aqueous solution. Besides, this biosensor required complicated manual procedures, which might lead to a great impact on its repeatability. Therefore, in the present study we combined electrochemical impedance spectra (EIS) analysis, urease catalysis, 3D printing with microfluidics to develop a microfluidic biosensor for faster detection of foodborne pathogens using *Listeria monocytogenes* as model. As shown in Fig. 1, the *Listeria* cells, the magnetic nanoparticles (MNPs) modified with the anti-*Listeria* monoclonal antibodies (MAbs), and the gold nanoparticles (AuNPs) modified with the anti-*Listeria* polyclonal antibodies (PAbs) and the urease were incubated in a fluidic separation chip to form the urease–AuNP–*Listeria*–MNP complexes. After successive washing with PBT (Tween-20 in 10 mM PB buffer, pH 7.2) and deionized water to remove the redundant AuNPs and the surplus conductive ions while the complexes were captured in the separation chip by applying a high gradient magnetic field, the urea prepared by deionized water was injected to resuspend the complexes and hydrolyzed under the catalysis of the urease on the complexes into ammonium ions and carbonate ions, resulting in an increase on the ionic strength of the solution. Finally, the solution was transported into a microfluidic detection chip housing an interdigitated microelectrode and its impedance change was measured by the IM6 electrochemical workstation (Zahner, Kronach, Germany) for quantitative detection of the *Listeria* cells.

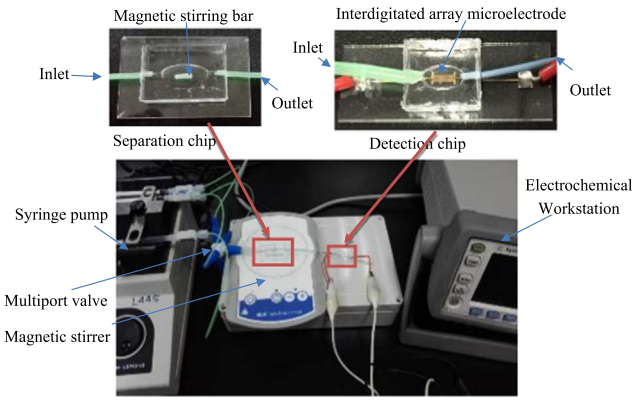


**Fig. 1.** The proposed microfluidic biosensor for sensitive detection of foodborne pathogens.

## 2. Materials and methods

### 2.1. Materials

The magnetic nanoparticles with the diameter of 180 nm were purchased from Allrun Nano (PM3-020, Shanghai, China) for immunomagnetic separation. The monoclonal and polyclonal antibodies against *Listeria monocytogenes* were obtained from Zodolabs Biotech (Nanchang, China) for specifically reacting with the *Listeria* cells. Gold chloride tri-hydrate ($HAuCl_4 \cdot 3H_2O$) purchased from Sigma Aldrich (St. Louis, MO, US) was used to synthesize the gold nanoparticles with the diameter of ~20 nm. Sodium citrate, streptavidin, biotin, urease (E.C.3.5.1.5, Type III, 15,000–50,000 units/g solid), urea ($NH_2CONH_2$), ammonium carbonate ($(NH_4)_2CO_3$), 1-(3-Dimethylaminopropyl)-3-ethylcarbodiimide hydrochloride (EDC · HCl), 2-(N-morpholino) ethanesulfonic acid (MES), and phosphate buffered saline solution (P5493, PBS, 10 times concentrated, diluted 10:1 by deionized water prior to use) were also purchased from Sigma Aldrich. Bovine serum albumin (BSA) from EM Science (Gibbstown, NJ, US) and polyethylene glycol (PEG) 20,000 from Merck (Darmstadt, Germany) were prepared in PBS for blocking. Tween-20 was purchased from Amresco (Solon, OH, US) for washing. Other reagents were of analytical grade and purchased from Sinopharm Chemical (Shanghai, China). All the solutions were prepared with deionized water produced by Advantage A10 from Millipore (Billerica, MA, USA).

The Silicone elastomer kit (SYLGARD 184) was purchased from Dow Corning (Auburn, MI, US) for fabricating poly(dimethoxy) silane (PDMS) channels. The printing material (Vero Whiteplus RGD835, Stratasys, Eden Prairie, MN) was used with the Objet30 3D printer to fabricate the molds of the channels. The glass slides were obtained from SAIL BRAND (7101, Jinan, China) and used to bond with the PDMS channels to fabricate the chips. The multiport valve purchased from (001118, Diba Industries, Danbury, CT) was used for switching the solutions to inject into the fluidic chips.

### 2.2. Fabrication of the separation and detection chips

The separation and detection chips were fabricated based on 3D printing and surface plasma bonding. First, the 3D drawings in . stl format were designed using the Solidworks software (Concord, MA, USA) and the molds were printed by the 3D printer with the accuracy of 100 μm in X axis and Y axis and 28 μm in Z axis. Prior to use of the molds, they were immersed in 5% NaOH for 30 min to thoroughly remove the surplus support material. The PDMS prepolymer and curing agent were mixed at the ratio of 8:1 for 30 min and degassed for 20 min in vacuum. Then, the mixture was

cured in the molds overnight at the curing temperature of 60 °C. Finally, the PDMS channels and the glass slide or the glass wafer with an interdigitated microelectrode were treated by surface plasma (Harrick Plasma, Ithaca, NY, US) and bonded to form the chips.

For the fluidic separation chip (Fig. 1.), the ellipse fluidic channel was designed with the length of 14 mm, the width of 6 mm, and the thickness of 4.5 mm, and a magnetic stirrer with the diameter of 1.6 mm and the length of 5 mm, containing an iron rod (~0.3 mm in diameter and ~3 mm in length), was embedded inside for mixing. For the microfluidic detection chip, the ellipse fluidic channel was designed with the length of 6 mm, the width of 3 mm and the thickness of 100 μm, and the microelectrode was embedded inside for impedance measurement. The microelectrode includes 25 pairs of digit electrodes with 10 μm digit width, 10 μm inter-digit spacing, and 3 mm digit length (see Fig. S1 in the Supplemental material).

### 2.3. Culture and enumeration of the bacterial cells

*Listeria monocytogenes* (ATCC13932, used as target bacteria) and *Escherichia coli* O157: H7 (ATCC43888, used as non-target bacteria) were stored at −20 °C with 15% glycerol and were revived by streaking on Luria-Bertani (LB) agar plates. They were first cultured in the LB medium (Aoboxing Biotech, Beijing, China) at 37 °C for 12–16 h with shaking at 180 rpm, respectively. Then, the cultures were 10-fold diluted by sterile PBS with 0.05% Tween 20 (v/v) to obtain the bacteria at the concentrations from $10^2$ to $10^5$ CFU/mL, respectively.

For bacterial enumeration, the bacterial samples were serially diluted with sterile PBS and 100 μL of the diluents were plated on the LB agar plates. The plates were then incubated at 37 °C for 22–24 h before the colonies were counted. The bacteria were enumerated in colony forming unit per milliliter (CFU/mL).

### 2.4. Preparation of the nanoparticles and chips

The monodisperse MNPs with the diameter of 180 nm were modified with the anti-*Listeria monocytogenes* monoclonal antibodies using EDC method and the gold nanoparticles with the diameter of ~20 nm were modified with the anti-*Listeria monocytogenes* polyclonal antibodies and urease, which have been reported in our previous publications (Chen et al., 2015).

A key to control the background noise is to minimize the non-specific adsorption in the fluidic separation chip. For this purpose, the chip was incubated with 1% BSA for 15 min prior to the injection of the solutions, and 0.05% Tween 20 were used in all the washing solutions. The effect of 0.05% Tween 20 on the non-specific adsorption was evaluated using $10^4$ CFU/mL of *Listeria* in both PBS and PBS with 0.05% Tween 20 to inject into the chips, incubate for 15 min, and collect the eluates for plating count.

### 2.5. Impedance measurement

Impedance measurements were performed using the interdigitated microelectrode fabricated at State Key Lab of Integrated Optoelectronics, Institute of Semiconductors, Chinese Academy of Science and the Zahner IM6 electrochemical workstation. For all the impedance measurements, an alternating sinusoidal potential with an amplitude of 5 mV, a direct-current bias of 0 V and a frequency range of 50 Hz–500 kHz was applied on the microelectrode.

### 2.6. Bacteria separation and detection

Bacteria separation and detection were based on immunomagnetic separation in the fluidic separation chip and impedance measurement in the microfluidic detection chip, respectively. First, 20 μL of the MAb modified MNPs and 5 μL of the PAb and urease modified AuNPs were added into 180 μL of *Listeria monocytogenes* at different concentrations ($10^2$–$10^5$ CFU/mL) and immediately injected at 2 mL/min into the separation chip. After the ellipse fluidic channel was filled with the mixture, it was incubated for 30 min with continuous magnetic stirring at 250 rpm to mix the MNPs and the AuNPs with the *Listeria* cells to prevent the MNPs from precipitation. After the MNP-*Listeria*-AuNP-urease complexes were formed, the separation chip was placed on a high gradient magnetic field with the strength of ~1.1 T for 90 s to capture the complexes onto the glass surface of the chip. Then, 2 mL of 10 mM PBT and 1.5 mL of deionized water were sequentially injected into the chip at 1 mL/min by switching the multiport valve to remove unbound AuNPs and residual conductive ions, respectively. Finally, the complexes were resuspended in 200 μL of 100 μM urea. After enzymatic catalysis for the optimal time of 5 min (see Fig. S2 in the Supplemental material), the complexes were magnetically separated for 90 s and the supernatant was transported into the detection chip for impedance measurement.

## 3. Results and discussions

### 3.1. Impedance and phase angle analysis of catalysate in microfluidic chip

This proposed microfluidic biosensor is based on quantitative determination of the catalysate (ammonium ions and carbonate ions) using the microfluidic chip with the interdigitated array microelectrode and the linear relationship between the impedance and phase angle of the catalysate (ammonium carbonate) and its concentration. Therefore, three parallel tests on different concentrations (1–100 μM) of ammonium carbonate, which was used to simulate ammonium ions and carbonate ions, at the presence of urea at the concentration of 100 μM were conducted using the microfluidic chip for proof of the concept. The electrochemical impedance spectra and the phase angle spectra of ammonium carbonate and urea at the frequency range of 50 Hz–500 kHz were shown in Fig. S3 in the Supplemental material. Fig. 2 (a) shows that a linear relationship between the impedance (Z) at the characteristic frequency of 3 kHz and the concentration of ammonium carbonate (c) ranging from 1 μM to 100 μM is obtained and can be described by $Z = -12{,}204 \log(c) + 64{,}091$ ($R^2 = 0.98$), verifying that the impedance of ammonium carbonate can be used to determine its concentration in the microfluidic chip. Fig. 2(b) shows that a linear relationship between the frequency (f) at the maximum phase angle and the concentration of ammonium carbonate (c) ranging from 1 μM to 100 μM is obtained and can be described by $f = 143.2c + 2274.3$ ($R^2 = 0.98$), verifying that the phase angle of ammonium carbonate can also be used to determine its concentration in the microfluidic chip.

To better understand the impedance data, the equivalent circuit reported in our previous study (see Fig. S4a in the Supplemental material), consisting of the resistance of the solution ($R_s$), the dielectric capacitance ($C_{di}$), and the double layer capacitance ($C_{dl}$), is used for the analysis of the electrochemical impedance spectra (Chen et al., 2015). The measured impedance and phase angle spectra of ammonium carbonate at 10 μM and the simulated spectra obtained from the equivalent circuit were shown in Fig. S4 (b) in the Supplemental material. The mean errors of the impedance magnitude and the phase angle were 4.5% with a maximum error of 9.9% and 6.5% with a maximum error of 14.6%, respectively, verifying the good fitting of the measured impedance and phase angle data to the equivalent circuit. Besides, the

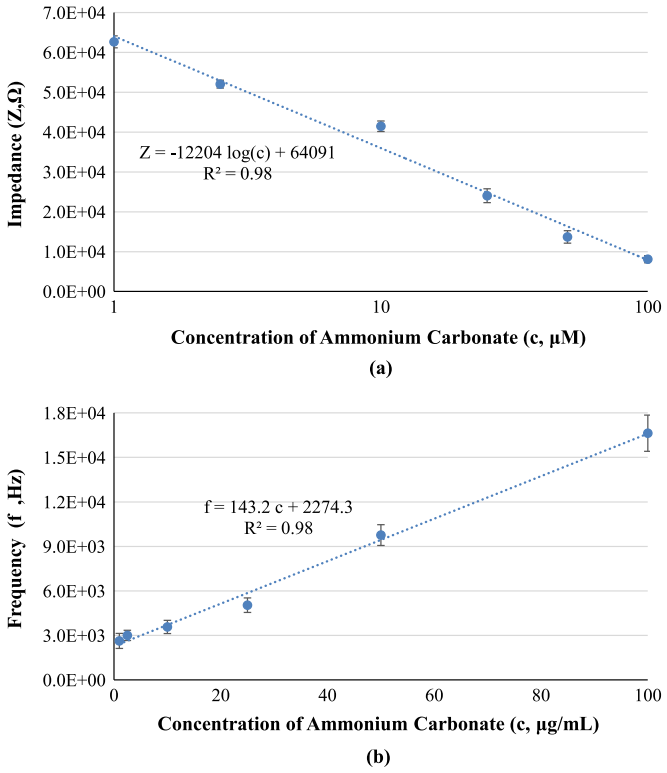


**Fig. 2.** (a) Linear relationship between the impedance of ammonium carbonate at the characteristic frequency of 3 kHz measured in the microfluidic chip and the concentration of ammonium carbonate (N=3); (b) Linear relationship between the frequency at the maximum phase angle and the concentration of ammonium carbonate (N=3).

**Table 1**
Contribution of the elements in the equivalent circuit to the impedance change in the detection of different concentrations of ammonium carbonate.

| $(NH_4)_2CO_3$ (μM) | $C_{di}$ (nf) | $\Delta C_{di}$[a] (%) | $R_s$ (kΩ) | $\Delta R_s$[a] (%) | $C_{dl}$ (pf) | $\Delta C_{dl}$[a] (%) |
|---|---|---|---|---|---|---|
| Control | 16.22 | – | 63.55 | – | 74.46 | – |
| 1 | 16.64 | 2.6 | 60.41 | −4.9 | 76.78 | 3.1 |
| 2.5 | 16.98 | 4.7 | 51.34 | −19.2 | 75.97 | 2.0 |
| 10 | 17.35 | 7.0 | 41.57 | −34.6 | 75.30 | 1.1 |
| 25 | 18.71 | 15.4 | 23.47 | −63.1 | 75.04 | 0.8 |
| 50 | 19.68 | 21.3 | 13.15 | −79.3 | 73.66 | −1.1 |
| 100 | 20.62 | 27.1 | 7.50 | −88.2 | 71.99 | −3.3 |

[a] $\Delta X=(X_s-X_c)/X_c$. $X$ stands for $C_{di}$, $R_s$ and $C_{dl}$; $X_s$ stands for the sample at different concentrations, $X_c$ stands for the control (urea).

measured impedance data at the frequency range of 50 Hz–500 kHz were analyzed using the ZSimpWin software to find the contribution of the elements to the impedance change in the detection of different concentrations of ammonium carbonate. The results are shown in Table 1, indicating that the double layer capacitance, $C_{dl}$, of ammonium carbonate at the concentrations of 1–100 μM only has ±5% changes compared to that of the control (urea), and the dielectric capacitance, $C_{di}$, has small increases from 2.6% at 1 μM to 27.1% at 100 μM, while the solution resistance, $R_s$, has obvious decreases from 4.9% at 1 μM to 88.2% at 100 μM. This verified that the resistance of ammonium carbonate decreases exponentially while the concentration increases.

Besides, the equivalent circuit was employed to calculate the phase angle for further investigating the effect of different concentrations of ammonium carbonate on the phase angle. The impedance ($Z$) of the proposed biosensor can be described by Eq. (1).

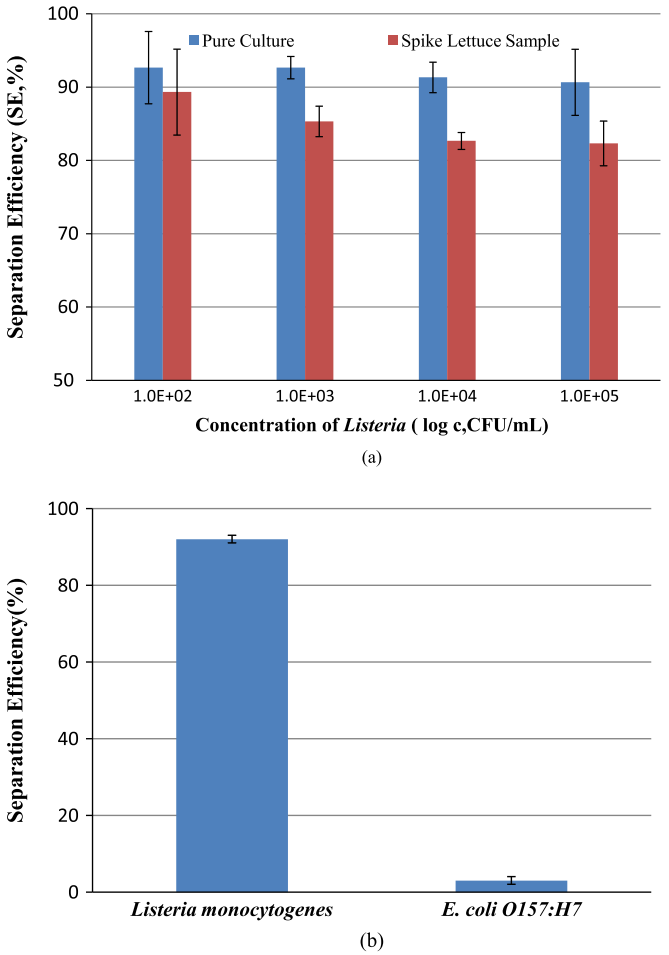


**Fig. 3.** (a) Separation efficiency of *Listeria monocytogenes* at the concentrations ranging from $1.6\times10^2$ to $1.6\times10^5$ CFU/mL in the pure cultures and from $2.4\times10^2$ to $2.4\times10^5$ CFU/mL in the spiked lettuce samples using the fluidic chip (N=3); (b) Separation efficiency of *Listeria monocytogenes* and *E. coli* O157:H7 at the concentration of $10^4$ CFU/mL in the pure cultures using the fluidic chip (N=3).

$$Z = Z_{re}+jZ_{im}Z_{re} = \frac{\omega R_s C_{dl}^2}{\omega^3 C_{dl}^2 C_{di}^2 R_s^2 + \omega(C_{dl}+C_{di})^2}$$

$$Z_{im}=-\frac{(\omega^2 R_s^2 C_{dl}^2 C_{di} + C_{dl} + C_{di})}{\omega^3 C_{dl}^2 C_{di}^2 R_s^2 + \omega(C_{dl}+C_{di})^2} \quad (1)$$

where $Z_{re}$ and $Z_{im}$ are the real and imaginary part of the impedance, respectively; $\omega=2\pi f$ is the angular frequency.

The phase angle of the impedance can be obtained as Eq. (2):

$$\varphi=\arctan(Z_{im}/Z_{Re}) = \arctan\left(-\frac{\omega^2 R_s^2 C_{dl}^2 C_{di} + C_{dl} + C_{di}}{\omega R_s C_{dl}^2}\right) \quad (2)$$

To obtain the characteristic frequency where the phase angle reached the maximum, the derivative of the phase angle was calculated and equal to zero.

$$\frac{d\varphi}{d\omega} = 0 \quad (3)$$

$$\omega = \sqrt{\frac{C_{dl}+C_{di}}{R_s^2 C_{dl}^2 C_{di}}} \quad (4)$$

From Eq. (4) and Table 1, when the concentration of ammonium carbonate increased, $C_{dl}$ almost remained unchanged, $C_{di}$ increased slowly and $R_s$ decreased fastly, which resulted in an increase on the characteristic frequency.

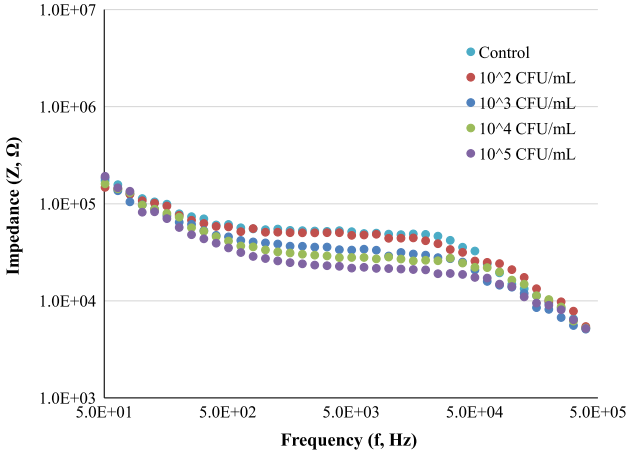


(a)

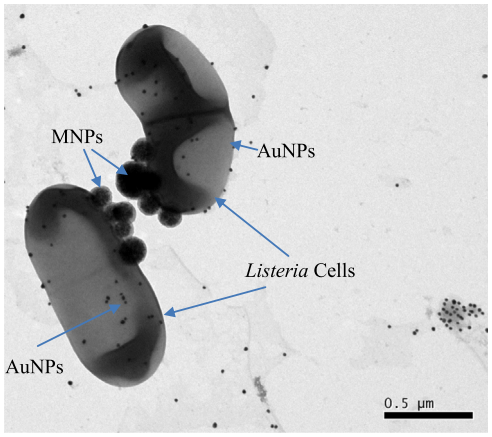


(c)

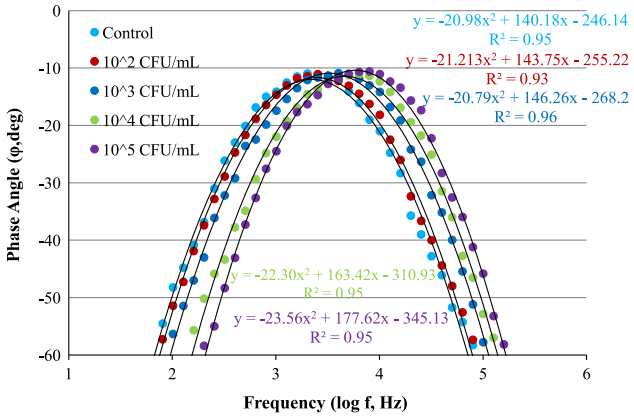


(b)

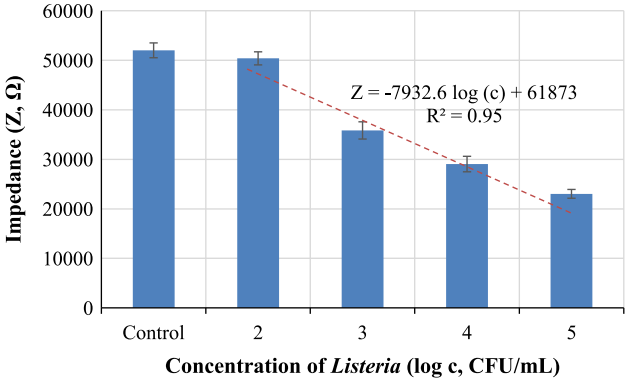


(d)

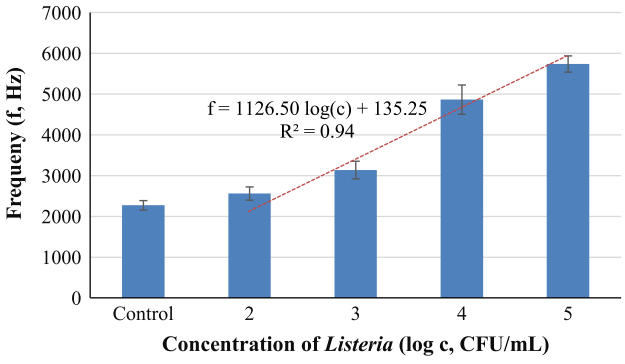


(e)

**Fig. 4.** (a) Impedance spectra of different concentrations of *Listeria* ranging from $1.6 \times 10^2$ to $1.6 \times 10^5$ CFU/mL; (b) Phase angle spectra of different concentrations of *Listeria* ranging from $1.6 \times 10^2$ to $1.6 \times 10^5$ CFU/mL; (c) TEM image of the MNP-*Listeria*-AuNP complexes; (d) Linear relationship between the impedance at the characteristic frequency of 3 kHz and the concentration of *Listeria* cells (N=3); (e) Linear relationship between the characteristic frequency at the maximum phase angle and the concentration of *Listeria* cells (N=3).

### 3.2. *Immunomagnetic separation of Listeria in fluidic chip*

The specific separation and efficient concentration of *Listeria* in the separation chip play an important role in the improvement of the specificity and sensitivity of this biosensor. Prior to the immunomagnetic separation in the chip, the chip was blocked by 1% BSA, and 0.05% Tween 20 was added into the *Listeria* samples. As shown in Fig. S5(a) in the Supplemental material, the non-specific adsorption of *Listeria* in the chip was reduced from 15% (without Tween 20) to 4% (with Tween 20). To further understand the effect of 0.05% Tween 20 on the separation of *Listeria*, the *Listeria* sample at $2.3 \times 10^4$ CFU/mL with and without 0.05% Tween 20 were used for magnetic separation. From Fig. S5(b) in the Supplemental material, it was found that 0.05% Tween 20 had no obvious effect on the separation of *Listeria* and the presence of 0.05% Tween 20 slightly improved the separation efficiency probably because Tween 20 could enhance the dispersivity of the MNPs for more efficient immunoreaction between the MAbs on the MNPs and the *Listeria* cells.

Three parallel tests were conducted for each concentration of

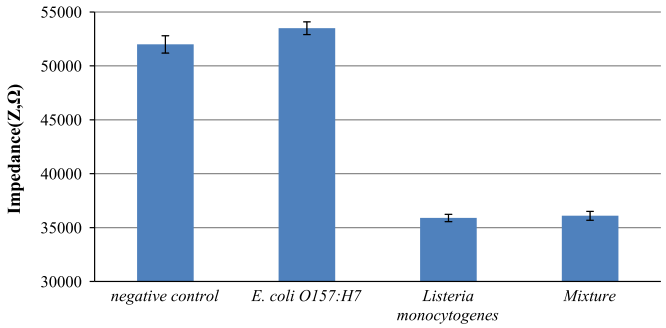


**Fig. 5.** The specificity of this proposed biosensor. The mixture of *Listeria* and *E. coli* O157:H7 at the concentration of $10^3$CFU/mL, only *E. coli* O157:H7 at the concentration of $10^3$CFU/mL, only *Listeria* at the concentration of $10^3$CFU/mL and the negative control were tested using this proposed biosensor.

*Listeria* ranging from $1.6 \times 10^2$ to $1.6 \times 10^5$ CFU/mL in the pure cultures and from $2.4 \times 10^2$ to $2.4 \times 10^5$ CFU/mL in the spiked lettuce samples. As shown in Fig. 3a, the separation efficiencies of all the concentrations of *Listeria* in the fluidic separation chip using the anti-*Listeria* MAb modified MNPs were ~93% for the pure cultures and ~80% for the spiked lettuce samples, which were basically consistent with the separation efficiencies of *Listeria* by conventional procedures reported in our previous studies (Chen et al., 2015). However, the total time for immunomagnetic separation in the fluidic separation chip was reduced from conventional ~90 min to current ~30 min. This might be attributed to two aspects: (1) the higher immuno-reaction efficiency between the MNPs and the *Listeria* cells due to the continuous magnetic mixing in the fluidic separation chip; (2) the higher capture efficiency of the *Listeria*-MNP complexes in the separation chip due to the application of a high gradient magnetic field for capturing the complexes against the glass surface of the separation chip. More importantly, when the complexes were firmly captured onto the glass surface of the separation chip, the washing solution could be continuously injected to remove the redundant AuNPs and the surplus conductive ions, where the tedious manual washing procedures were neglected. Besides, the separation efficiency of non-target bacteria (*E. coli* O157: H7) at the concentration of $4 \times 10^4$ CFU/mL in the pure culture was less than 3% (see Fig. 3b), indicating that the immunomagnetic separation had a good specificity and also was comparable with previous reports (Chen et al., 2015; Mao et al., 2016).

### 3.3. Detection of Listeria in microfluidic chip

The impedance of the catalysate (ammonium ions and carbonate ions) at the presence of urea relies on the concentration of the urease on the MNP-*Listeria*-AuNP-urease complexes. Three parallel tests on pure *Listeria* at the concentrations of $10^2$–$10^5$ CFU/mL were conducted using this proposed biosensor. The impedance spectra and phase angle spectra for different concentrations of *Listeria* cultures were shown in Fig. 4(a) and (b). Besides, TEM imaging was used to check the successful forming of the MNP-*Listeria*-AuNP-urease complexes (see Fig. 4c). It was found that the impedance decreased and the characteristic frequency shifted rightward while the concentrations of *Listeria* increased. The impedance responses in the aspects of both magnitude and phase angle to different concentrations of *Listeria* were observed to have regular trends, and the impedance magnitude at the characteristic frequency of 3 kHz and the characteristic frequency at the maximum phase angle were plotted for different concentrations of the *Listeria* cells and shown in Fig. 4d and e. This proposed biosensor owned a linear relationship between the impedance (Z) at the characteristic frequency and the concentration of *Listeria* (c) ranging from $1.6 \times 10^2$ to $1.6 \times 10^5$ CFU/mL, which can be described as $Z = -7932.6 \log(c) + 61{,}873$ ($R^2 = 0.95$), and a linear relationship between the characteristic frequency (f) at the maximum phase angle and the concentration of *Listeria* (c) as well, which can be described as $f = 1126.50 \log(c) + 135.25$ ($R^2 = 0.94$). The low detection limit of the biosensor was determined by three times of signal-to-noise ratio to be $1.6 \times 10^2$ CFU/mL.

### 3.4. Specificity of the microfluidic impedance biosensor

The specificity of this proposed biosensor depends on the anti-*Listeria* monoclonal and polyclonal antibodies. *E. coli* O157: H7 were used as the non-target bacteria to test its specificity. Three parallel tests on the mixture of *Listeria* and *E. coli* O157: H7 at the concentration of $10^3$CFU/mL, only *E. coli* O157: H7 at the concentration of $10^3$CFU/mL, and only *Listeria* at the concentration of $10^3$CFU/mL were conducted. As shown in Fig. 5, the results showed that the impedance of the mixture of *Listeria* and *E. coli* O157: H7 (36.1kΩ) was close to that of only *Listeria* (35.9kΩ) and the impedance of only *E. coli* O157: H7 (53.5kΩ) was close to that of the negative control (52.0kΩ). Besides, some salt ions, such as NaCl, $NH_4Cl$ and $NaHCO_3$ at the concentration of ~0.1M, were also mixed with the *Listeria* cells at the concentration of $10^3$CFU/mL and tested using this biosensor. The impedance spectra of *Listeria* with and without the salt ions almost overlapped because the salt ions were washed out in the magnetic separation and washing procedures. The tests on both *E. coli* O157: H7 and salt ions indicated that this proposed biosensor had a good specificity.

To evaluate the applicability of this proposed biosensor, different concentrations of *Listeria* in the spiked lettuce samples were magnetically separated using the proposed separation chip and detected using the proposed detection chip. Three parallel tests for each concentration were conducted and the recoveries ranged from 82.1% to 89.6%, indicating the applicability of the proposed biosensor.

## 4. Conclusions

This study presented a microfluidic biosensor combining immunomagnetic separation, impedance and phase angle analysis and urease catalysis for rapid and sensitive detection of foodborne pathogens using *Listeria monocytogenes* as model and an antibody immobilization-free interdigitated microelectrode as transducer. We demonstrated that this proposed biosensor was capable of detecting *Listeria* as low as $1.6 \times 10^2$ CFU/mL in 1 h based on either the phase angle shift analysis or the impedance change analysis. More importantly, this microfluidic biosensor has shown the potential for online, automatic and sensitive bacteria separation and detection. The merit of this method might be easily extended for the detection of other foodborne pathogens and biological targets and it is promising to develop a sensitive, rapid and low-cost microfluidic device.

## Acknowledgments

This study was supported in part by Science and Technology Support Plan of Hebei Province, China (No. 16275508D), and Special Fund for Agro-Scientific Research in the Public Interest (No. 201303045).

## Appendix A. Supplementary material

Supplementary data associated with this article can be found in the online version at http://dx.doi.org/10.1016/j.bios.2016.07.071.

## References


Chen, Q., Lin, J., Gan, C., Wang, Y., Wang, D., Xiong, Y., Lai, W., Li, Y., Wang, M., 2015. Biosens. Bioelectron. 74, 504–511.

Chen, Z., Ren, X., Meng, X., Chen, D., Yan, C., Ren, J., Yuan, Y., Tang, F., 2011. Biosens. Bioelectron. 28 (1), 50–55.

Ghosh Dastider, S., Barizuddin, S., Yuksek, N.S., Dweik, M., Almasri, M.F., 2015a. J. Sens., 2015.

Ghosh Dastider, S., Barizuddin, S., Yuksek, N.S., Dweik, M., Almasri, M.F., 2015b. J. Sens. 2015, 1–8.

Hernandez, R., Valles, C., Benito, A.M., Maser, W.K., Rius, F.X., Riu, J., 2014. Biosens. Bioelectron. 54, 553–557.

Kanayeva, D.A., Wang, R., Rhoads, D., Erf, G.F., Slavik, M.F., Tung, S., Li, Y., 2012. J. Food Prot. 75 (11), 1951–1959.

Larou, E., Yiakoumettis, I., Kaltsas, G., Petropoulos, A., Skandamis, P., Kintzios, S., 2013. Food Control 29 (1), 208–212.

Lee, W., Kwon, D., Chung, B., Jung, G.Y., Au, A., Folch, A., Jeon, S., 2014. Anal. Chem. 86 (13), 6683–6688.

Lin, J., Wang, R., Jiao, P., Li, Y., Li, Y., Liao, M., Yu, Y., Wang, M., 2015. Biosens. Bioelectron. 67, 546–552.

Liu, Q.-L., Yan, X.-H., Yin, X.-M., Situ, B., Zhou, H.-K., Lin, L., Li, B., Gan, N., Zheng, L., 2013. Molecules 18 (10), 12675–12686.

Mao, Y., Huang, X., Xiong, S., Xu, H., Aguilar, Z.P., Xiong, Y., 2016. Food Control 59, 601–608.

Mclinden, T., Sargeant, J.M., Thomas, M.K., Papadopoulos, A., Fazil, A., 2014. BMC Public Health 14 (12), 1–12.

Miranda, O.R., Li, X., Garcia-Gonzalez, L., Zhu, Z.J., Yan, B., Bunz, U.H., Rotello, V.M., 2011. J. Am. Chem Soc. 133 (25), 9650–9653.

Scharff, R.L., 2012. J. Food Prot. 75 (1), 123–131.

Sun, Y.H., Kong, R.M., Lu, D.Q., Zhang, X.B., Meng, H.M., Tan, W., Shen, G.L., Yu, R.Q., 2011. Chem. Commun. 47 (13), 3840–3842.

Tang, Y., Li, Z., Luo, Q., Liu, J., Wu, J., 2016. Biosens. Bioelectron. 79, 715–720.

Varshney, M., Li, Y., 2009. Biosens. Bioelectron. 24 (10), 2951–2960.

Wang, Y., Liu, B., 2009. Biosens. Bioelectron. 24 (11), 3293–3298.

Wang, Y., Knoll, W., Dostalek, J., 2012. Anal. Chem. 84 (19), 8345–8350.

Xue, J., Zhang, W., 2013. Food Control 30 (1), 311–317.